	Scar Baseline distribution							
	Right-Left [mm]		Inferior-Superior [mm]		Posterior-Anterior [mm]		n Fr	TOT Treatment Time [min]
	median	iqr	median	iqr	median	iqr		
P 1	0.16	1.11	-0.24	0.93	-1.27	1.43	8	96.29
P 2	1.32	3.06	2.27	8.53	2.84	8.12	6	83.75
P 3	0.44	0.86	-0.29	0.72	-1.72	1.36	5	61.62
P 4	0.16	0.62	-1.32	2.18	-2.60	3.09	12	152.01
P 5	0.45	1.22	-1.31	1.45	-0.46	1.41	9	120.66
P 6	0.55	1.58	-0.04	1.01	-0.24	0.90	3	42.08
P 7	-0.74	1.01	-0.74	1.78	-1.19	3.24	4	63.50
P 8	1.46	2.50	-0.88	2.17	-1.65	1.93	5	71.45
P 9	-0.53	0.92	0.18	1.68	-0.67	1.68	9	126.75
P 10	0.00	1.08	-2.48	1.50	-2.22	2.16	4	61.46
P 11	0.45	1.10	-0.42	1.24	-0.70	0.81	6	97.79
P 12	-0.01	1.22	0.55	1.73	-1.43	1.42	8	127.15
P 13	-0.17	0.80	-2.00	3.44	-2.19	2.95	8	125.17
P 14	0.13	1.02	0.18	1.79	-1.37	1.27	4	69.19
P 15	-0.59	1.35	-4.34	1.37	-3.31	2.62	6	100.50
P 16	-0.10	1.60	-0.06	1.02	-0.28	1.36	3	51.52
P 17	1.20	0.76	-0.03	2.08	-0.51	1.38	2	38.34
P 18	0.26	0.70	-1.12	1.48	-1.58	1.64	11	195.55
P 19	0.02	2.11	0.05	2.08	-0.35	1.64	5	93.46
P 20	-0.05	1.21	0.38	1.70	0.09	1.05	2	37.39
TOT	**0.11**	**1.18**	**-0.56**	**1.99**	**-1.18**	**2.00**	**120**	**1815.62**

Iqr = inter-quartile range; n FR = number of fraction

Conclusion: Respiratory and non-respiratory motion during prolonged treatment induces significant position errors. Resulting CTV to Planning Target Volume (PTV) margins are within the 5 mm isotropic expansion generally used in clinic. Non-invasive continuous monitoring of intra-fraction motion should be implemented for an accurate definition of PTV.

EP-1754

The accuracy of ExacTrac X-ray intra-fraction verification at non-zero couch rotation

D.L.J. Barten[1], N.D. Sijtsema[1], M. Zahir[1], J.P. Cuijpers[1]
[1]*VUMC, Radiotherapie, Amsterdam, The Netherlands*

Purpose or Objective: Submillimeter accuracy of patient positioning is mandatory in stereotactic radiation therapy (SRT), since a high dose per fraction is given to relatively small lesions using tight PTV margins. SRT treatment techniques normally use couch rotations to achieve optimal irradiation. In frameless SRT intrafraction positioning verification at non-zero couch angles is recommended to ensure correct dose delivery. In this study the accuracy of the frameless ExacTrac X-Ray verification system at non-zero couch angles was assessed.

Material and Methods: An Alderson head phantom with a hidden marker was immobilized in a BrainLAB frameless mask on the Novalis Tx system. The phantom was positioned using the ExacTrac X-Ray system at couch angle 0°. For 13 different couch angles the phantom position was determined using the i) infrared (IR) optical markers, ii) X-ray verification imaging and iii) MV images taken from the AP direction. In the latter only deviations in the couch rotation plane were measured, assuming negligible deviations in the vertical direction. The Winston-Lutz test was performed to validate this assumption. The AP-MV imaging was used as the golden standard and was compared with the ExacTrac IR and X-ray results for each couch angle to determine the accuracy of the ExacTrac system. All data were relative to couch angle 0° and calculated in the Linac coordinate system. A one sample T-test was performed to determine statistically significant ($p<0.05$) differences between the systems.

Results: Deflection of the couch in the vertical direction was within 0.23 mm at couch angle 0° and variation at other couch angles is less than 0.1mm. X-Ray verification at different couch angles showed significant differences with the AP-MV imaging of 0.23±0.12mm and 0.30±0.21mm on average for longitudinal and lateral direction respectively. Maximum deviations between AP-MV imaging and ExacTrac X-ray were found at couch angle 30° of 0.63mm in lateral and 0.50mm in longitudinal direction. Verification with the IR markers shows larger deviations than the X-ray verification. Largest mean deviations for longitudinal and lateral direction were -1.55mm (at couch angle 270°) and 1.14mm (at couch angle 90°).

Conclusion: X-Ray verification at non-zero couch angles using the ExacTrac system is sufficiently accurate to be used in SRT. Deviations in X-Ray verification were largest at couch angle 30° but this will be of minimal importance clinically, since in non-coplanar SRT treatment techniques multiple couch angles are used. The IR system shows deviations that exceed accuracy requirements for SRT.

EP-1755

Visualization of respiratory and cardiac motion via TomoTherapy exit detector fluence

N. Corradini[1], P. Urso[1], C. Vite[1]
[1]*Clinica Luganese, Radiotherapy Center, Lugano, Switzerland*

Purpose or Objective: To demonstrate that respiratory and cardiac motion is observable and quantifiable on the CT detector during TomoDirect breast treatments.

Material and Methods: A preliminary study for motion management in breast radiotherapy was performed using the exit detector fluence of tangential static IMRT fields on TomoTherapy. Two patients in treatment for left breast cancer were selected randomly for study. After their radiotherapy treatments, the raw pulse-by-pulse detector data was downloaded from the CT detector for analysis. The pulse-by-pulse detector data is sampled at a frequency of 300 Hz. The exit detector channels with fluences corresponding to the breast and heart surfaces were identified within the recorded treatment sinograms. These channels' fluences were then investigated at the temporal projections in which respiratory and cardiac motion were expected (Figures 1a-b).

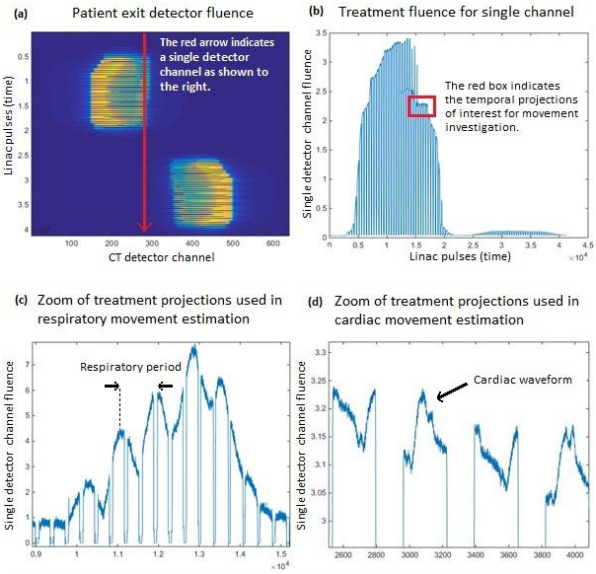

Figure 1. (a) Example of the the pulse-by-pulse exit detector fluence for a breast patient. (b) Example of a single fluence profile for an entire patient treatment. (c) Zoom of single channel fluence at the breast surface used for respiratory motion estimation. (d) Zoom of single channel fluence at the heart surface used for cardiac motion estimation.

Results: Sinusoidal and waveform variations in fluence were observed where respiratory and cardiac motion was expected. The sinusoidal motion recorded on the detector data at the expected breast surface averaged a period of 2.8 ± 0.1 sec during the 4 fractions that were analyzed. The cardiac waveform motion recorded on the detector data at the expected heart surface averaged a rate of 86.4 ± 2.0 bpm during the 3 fractions that were investigated (Figures 1c-d).

Conclusion: The fluence variations we have observed on the pulse-by-pulse detector data would fit reasonably within respiratory and cardiac motion. These preliminary results are indicative of the ability for visualization and quantification of